Angervuori, Jouko; Wichman, R.

A Closed-Form Approximation of the SIR Distribution in a LEO Uplink Channel

Published in:
2022 IEEE Globecom Workshops (GC Wkshps)

DOI:
10.1109/GCWkshps56602.2022.10008485

Published: 12/01/2023

Document Version
Peer-reviewed accepted author manuscript, also known as Final accepted manuscript or Post-print

Please cite the original version:
Angervuori, J., & Wichman, R. (2023). A Closed-Form Approximation of the SIR Distribution in a LEO Uplink Channel. In *2022 IEEE Globecom Workshops (GC Wkshps)* (pp. 856-861). IEEE.
https://doi.org/10.1109/GCWkshps56602.2022.10008485

A Closed-Form Approximation of the SIR Distribution in a LEO Uplink Channel

Ilari Angervuori
School of Electrical Engineering
Aalto University
02150 Espoo, Finland
ilari.angervuori@aalto.fi

Risto Wichman
School of Electrical Engineering
Aalto University
02150 Espoo, Finland
risto.wichman@aalto.fi

***Abstract*—The Low Earth Orbit (LEO) satellite networks will improve the quality of future communication networks. The rapid expansion of LEO networks brings up considerations of man-made interference from terrestrial networks or other LEO terminals. Especially the future terrestrial networks will cause interference in satellite receivers as higher frequency bands will be utilised in the emerging 5G and beyond networks. We study the distribution of signal-to-interference ratio (SIR) in a narrow beam LEO satellite receiver affected by a dense heterogeneous set of interfering transmitters. We propose that the distribution of interference power approximates the Gaussian distribution for the positive values. Furthermore, we suggest that the distribution of SIR follows the gamma distribution. We use the tools of stochastic geometry and derive the location, shape, and scale parameters for the distributions of interference and SIR. The parameters depend on the amount of interfering transmitters inside the receiving satellite's 3 dB footprint, the transmitting powers, and the slow and fast fading conditions.**

I. Introduction

The emerging Low Earth Orbit (LEO) satellite communication will play a vital part in the future networks supplementing the traditional terrestrial networks. The advantages of LEO networks include low latency and immunity to natural or man-made calamities. In addition, they can provide reliable and fast connections to remote parts of the world.

LEO networks work in high frequencies up to mm-waves. Today such frequencies have been allocated for satellite communications, but in the future, 5G and beyond technologies will utilize these high-frequency bands as well. In addition, the amount of other terrestrial-satellite terminals will increase as the future LEO networks will potentially include thousands, or even tens of thousands of satellites. These facts bring up a question about the interference in a satellite uplink in the presence of a heterogeneous set of interfering transmitters.

We will apply the tools from stochastic geometry to study the interference in a terrestrial-satellite uplink, where the satellite will experience additive interference power from multiple overlapping classes of interferers inside its field of view. We assume that each class of interfering transmitters is Poisson distributed on the Earth. The interferers experience slow fading and Rician fast fading conditions. We propose that the statistical interference power approximates the Gaussian distribution for the positive values. Furthermore, we propose that the signal-to-interference ratio (SIR) follows approximately the gamma distribution. We derive the parameters for the distributions based on the analysis of ratio distributions and second-moment matching. The approximation is especially applicable for high densities of interferers.

A. Related works and motivation

David Middleton's seminal paper [1] derives closed-form approximations for a statistical-physical interference waveform in three qualitatively different situations characterized by the interference's impulsiveness. These distributions are often referred to as Middleton class A, B, and C distributions. As a generic source of interference, Poisson point process (PPP) has been studied, for example, in [2]-[3][4]. In these papers, the distribution of instantaneous in-phase and quadrature components is expressed as the alpha-stable distribution [5]. In [6] Gaussian, Middleton class A and alpha-stable distributions were studied in ad-hoc and cellular networks to model the interference. Using second-order moment matching [7] proposes a gamma distribution approximation for the distribution of interference power in a heterogeneous terrestrial cellular network – this approximation is possible by assuming a non-singular path-loss function. In [8], a semi-analytical expression for the tail probabilities of SIR was obtained.

In these papers, it turns out that modeling interference by Gaussian statistics often works poorly because the tails of Gaussian distribution decay fast. However, in satellite communications, the topology of the Earth facilitates a qualitatively different setting, and the terrestrial models cannot be used as such. Contrary to terrestrial networks, the distribution of interference is not heavy-tailed as the interferers are concentrated in a small area at a high distance inside the receiver's footprint, and the source domain of interference can be considered even point-like in the case of narrow state-of-the-art beamforming. Thus, the path-loss function is constant (in contrary to a path-loss function with a singularity), and the expected interference power is well defined. The aggregate interference power will follow the normal distribution with the parameters derived in this paper.

Stochastic geometry has not been used to model satellite networks until recently. Analysis of interference in a satellite-terrestrial downlink is provided in [9], whereas [10] studies of uplink and downlink coverage probabilities in inclined LEOs. However, contrary to this paper, both [9], and [10] use the binomial process instead of the Poisson point process. The work in [11] used the Poisson process to model interfering transmitters in a terrestrial-satellite uplink evaluating data rates under Rician fading conditions. However, the analysis relies on a rather cumbersome numerical inversion of the Laplace transform. An analysis of data rates in a terrestrial-satellite uplink applying PPP theory is presented in [12]. None of these papers gives closed-form expressions for the distribution of interference or SIR. A survey on possible implementations of future ultra-dense satellite networks can be found in [13].

B. Our contribution

We apply the PPP analysis to satellite communications and exploit the fact that the satellite's main lobe is small with state-of-the-art beamforming technologies, and the distance to the satellite can be approximated to be equal to all transmitters inside a footprint. By this assumption, we are able to characterize the distribution of SIR by the well-known gamma distribution. First, we derive the Laplace transform of the interference from multiple classes of interferers assuming that the interferers are Poisson distributed on Earth's surface. Each class of interferers has distinct fading conditions, mean transmitting powers, density, and antenna pattern. From the Laplace transform, we conclude that the distribution of the additive interference can be approximated by Gaussian distribution for positive values with the parameters we derive. Based on this Gaussian approximation, we derive the distribution of SIR in the terrestrial-satellite transmission, where a terrestrial test transmitter transmits from an Earth station to a satellite at a definite elevation angle and altitude. We validate the approximation by comparing the gamma distribution approximation to Monte Carlo simulated distributions with a Gaussian antenna gain. We will notice that the approximation is very good with higher densities of transmitters and reasonable with lower densities.

Analysis in this paper provides insight and a closed form distribution that can be used to model the SIR in further studies of LEO networks.

In case of dense satellite constellations, the locations of the satellites can be modeled as a point process, see [9] - [12]. Hence, the analysis presented in this paper works with minor modifications in a satellite-terrestrial downlink if the density of the interfering satellites is high and the receiver's antenna pattern is narrow enough.

II. System Model

We consider an interference-limited terrestrial-satellite uplink transmission. A test transmitter (TX) is transmitting to a LEO satellite receiver (RX) with a mean transmitting power p_{TX}. The receiving satellite is at a definite elevation angle w.r.t. the test transmitter, and its boresight faces the test transmitter. The test transmitter boresight steers towards the satellite. Inside the field of view of the satellite, there are interfering transmitters. Assuming that the transmitters are

Glossary of principal symbols	
Symbol	Explanation
d	Distance between the test transmitter and the satellite
h	Altitude of the satellite
$\Phi^{(i)}$	Poisson point process of class i
$\lambda_{3dB}^{(i)}$	Mean number of class i interferers inside the satellite 3 dB footprint
$\lambda_{km}^{(i)}$	Mean number of class i interferers per square kilometer
$\lambda^{(i)}$	$3/2 \cdot \lambda_{3dB}^{(i)}$
$P_I^{(i)}$	Typical virtual power (power after the fading gain) of an interfering transmitter in class i
$p_I^{(i)}$	Mean power of an interfering transmitter in class i
$K_I^{(i)}$	Rician parameter of the interferer class i
$L^{(i)}$	Response function of class i transmitters
I	Aggregate interference
μ_I	Mean of the interference
s_I^2	Variance of the interference
p_{TX}	Mean power of the test transmitter
ν_{TX}	LOS component of the test transmitter
σ_{TX}	Scattered path component of the test transmitter

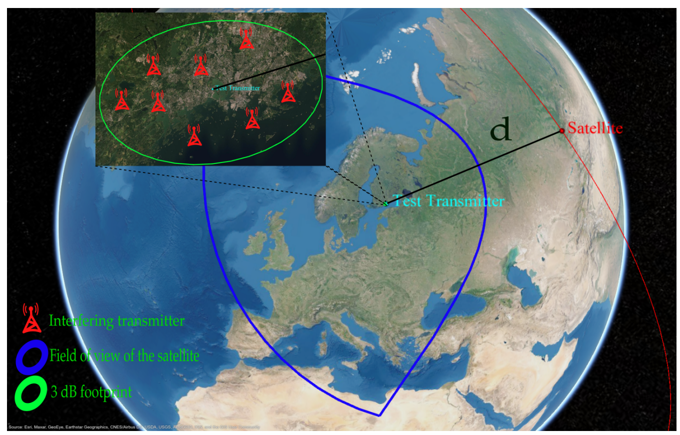

Fig. 1. System model

independently distributed on Earth, we assume that they follow the Poisson point process. That is, the number of interfering transmitters inside the satellite footprint is Poisson distributed. We treat the interference from the interfering transmitters as additive noise, i.e., the transmitted signals are uncorrelated. We do not consider any interference cancellation techniques. All interferers radiate omni-directionally.

A. Poisson Point Process

The interfering transmitters $x_i \in \Phi$ are Poisson distributed on Earth surface $\mathcal{E}$ according to the Poisson point process (PPP) Φ. Vaguely, Φ is a *completely* independent and identically distributed random set of points in the manifold $\mathcal{E}$. Equivalently, if $\Lambda(A)$ denotes a (deterministic) measure of a set $A \subset \mathcal{E}$, Φ can be defined as a random measure s.t. $\Phi(A)$ is Poisson distributed and $\mathbb{E}\Phi(A) = \Lambda(A)$ for all measurable A.

B. Response function

Response function $L(\cdot)$ maps a variable $d \in \mathbb{R}^n$ to a positive real number $\mathbb{R}$. In this work, d represents the distance between the satellite and the test transmitter, and L is a path-loss function

$$L(d) = (Ad)^{-\alpha}, \tag{1}$$

where $A \in \mathbb{R}_+$, and the path-loss power exponent $\alpha \in \mathbb{R}_+$. In other applications, the response function could depend, for example, also on time.

C. Fading

All transmitters experience Rician fading with Rician parameter $K = \nu^2/(2\sigma^2)$, where ν^2 is the power in the line-of-sight (LOS) component and $2\sigma^2$ is the power received from the scattered paths. Consequently, the virtual power seen in the receiver after the fading is generalized noncentral chi-squared distributed.

D. Signal to interference ratio

We define the signal-to-interference ratio with interfering transmitters $\{x_j^{(i)}\}_{j=1}^M$ in point processes $\{\ \Phi^{(i)}\}_{i=1}^N$ as

$$\text{SIR} = \frac{L(d)P_{\text{TX}}}{I} = \frac{L(d)P_{\text{TX}}}{\sum_{x_j^{(i)} \in \cup_i \Phi^{(i)}} P_j^{(i)} L^{(i)}(d_j)}, \tag{2}$$

where $d = d(x_0)$ is the distance from the test transmitter (at x_0) to the satellite, P_{TX} is the virtual power (power after the fading gain) of the test transmitter. Power $P_j^{(i)}$ denotes the virtual power of a transmitter j belonging to the class i, and $L^{(i)}(d_j)$ denotes the path-loss function of the class i at distance d_j.

We assume that all transmitting powers $\{P_j^{(i)}\}_{j=1}^M$ in a class are independent identically distributed (i.i.d.). Often we refer to a typical power of an interferer of class i as $P_I^{(i)}$. The mean power of a typical transmitter is denoted by $p_I^{(i)}$.

E. Shadowing

Transmitters are shadowed at probability S. If the original point process is of density λ, the shadowed transmitters form a Poisson point process of density $S \cdot \lambda$, and the non-shadowed transmitters form a PPP of density $(1 - S)\lambda$. This rather intuitive result is a consequence of the thinning theorem of the PPP [14].

F. Weather model and Doppler shift

We consider that the receiver's antenna beam is narrow, and the interferers are essentially very close to each other. Thus, the weather conditions are approximately equal to all transmitters including the test transmitter and cancel each other in the definition of SIR 2. Similarly, the Doppler shift is approximately equal to the test transmitter's Doppler shift, and hence does not have any effect on the aggregate interference power even after the receivers bandpass filter.

G. Receiver antenna gain

When φ_{RX} is the width of the 3 dB beam, we approximate the receiving antenna gain by a Gaussian beam

$$G_{\text{RX}}(\varphi) = 2^{-\varphi^2/\varphi_{RX}^2} \text{ for } \varphi \leq \varphi_{\text{RX}} \leq \pi/2, \tag{3}$$

where φ denotes the angle w.r.t. the antenna boresight.

III. Analysis

A. Distribution of the interference

The Laplace transform $\mathcal{L} : \mathbb{C} \to \mathbb{C}$ of the interference I from a point process Φ is given by [14], [11]:

$$\mathcal{L}_I(z) := \mathbb{E}\left[e^{-Iz}\right] = e^{-\int_{\mathcal{E}} \left(1 - \mathcal{L}_{P_I}(L(d(x))G_{RX}(\varphi(x))z)\right)\Lambda(dx)}, \tag{4}$$

where P_I denotes the typical virtual power of an interferer.

In case of a well steered narrow antenna beam, we can approximate that all transmitters are at an equal distance d from the satellite. Then $\mathcal{E}$ reduces to a single point x_0 of mass $\Lambda(x_0) := \lambda$ and (4) gets the form;

$$\mathcal{L}_I(z) = e^{-\lambda\left(1 - \mathcal{L}_{P_I}(L(d)z)\right)}. \tag{5}$$

In this paper, we define $\lambda := 3/2 \cdot \lambda_{3dB}$, where λ_{3dB} is the mean number of transmitters inside the satellite's 3 dB footprint, and $3/2$ is an empirical parameter that compensates the energy from the side lobes. Should the satellite be in the zenith, the mean number of interferers can be calculated by the area formula of a spherical cap: $\lambda_{3dB} = \lambda_{km} 2\pi R_\oplus^2 (1 - \cos(\theta))$, where θ denotes the central angle of the 3dB footprint and λ_{km} is the mean number of transmitters per square kilometer. For lower elevation angles of the satellite, the footprint is elliptical and the expressions are more complicated. We leave the geometrical considerations out of the scope of this paper, and λ_{3dB} will be always given.

We know that the Laplace transform of the non-central chi-squared distributed faded power variable is given by

$$\mathcal{L}_{P_I}(z) = \frac{e^{-\frac{\nu_I^2 z}{1+2z\sigma_I^2}}}{1 + 2z\sigma_I^2}. \tag{6}$$

Substituting (6) to (5) and applying a first degree Taylor expansion to the exponent yields

$$\mathcal{L}_I(z) \approx \exp\left\{-\lambda p_I L(d)z + 1/2\lambda L(d)^2 \frac{2 + 4K_I + K_I^2}{(1 + K_I)^2} p_I^2 z^2\right\}. \tag{7}$$

where $K_I = \nu_I^2/(2\sigma_I^2)$ is the Rician parameter of an interferer.

One can observe that for $z = -it \in \mathbb{C}$,

$$\mathcal{L}_I(-it) \approx \exp\left\{\lambda p_I it L(d) - 1/2\lambda L(d)^2 \frac{2 + 4K_I + K_I^2}{(1 + K_I)^2} p_I^2 t^2\right\}, \tag{8}$$

which is the characteristic function $t \mapsto \varphi(t) = \mathcal{L}(-it)$ of the normal distribution with mean $\mu_I = \lambda p_I$ and variance $s_I^2 = \lambda(2 + 4K_I + K_I^2)/(1 + K_I)^2 pI^2$.

For the Laplace transform it holds that $\mathcal{L}_{I^{(1)}+I^{(2)}}(s) = \mathcal{L}_{I^{(1)}}(s)\mathcal{L}_{I^{(2)}}(s)$ for all s. Thus, it is easy to see from (8) that in case of multiple classes of point processes $\{\Phi^{(i)}\}$:

Proposition 1 (Distribution of I)**.** *The interference I is distributed as the* ***normal distribution*** *$\mathcal{N}(\mu_I, s_I^2)$ with mean*

$$\mu_I = \sum_i \lambda^{(i)} L^{(i)}(d) p_I^{(i)} \tag{9}$$

and variance

$$s_I^2 = \sum_i \lambda^{(i)} L^{(i)}(d)^2 \frac{2 + 4K_I^{(i)} + (K_I^{(i)})^2}{(1 + K_I^{(i)})^2} (p_I^{(i)})^2, \tag{10}$$

where $\lambda^{(i)}, L^{(i)}, K_I^{(i)}, p_I^{(i)}$ are the density, response function, Rician parameter and mean transmitting power of the interferer class i, respectively.

Finally, let us make the following observation that comes later III-D1 into use in a special case of a Rayleigh faded test transmitter signal: for $s = t \in \mathbb{R}_+$, only the first term in (8) is dominating in the exponent and

$$\mathcal{L}_I(t) \approx \exp\left\{ -\sum_i \lambda^{(i)} L^{(i)}(d) p_I^{(i)} t \right\}. \tag{11}$$

B. Inverse distribution of the interference

It can be shown that the inverse of a Gaussian distributed random variable is approximately Gaussian under certain conditions [15]. We propose a similar approximation by a log-normal distribution. The following proposition applies under the conditions presented in this paper, and it can be verified, e.g., by Monte Carlo simulations.

Proposition 2 (Inverse of I)**.** *Let $I \sim \mathcal{N}(\mu_I, s_I^2)$, then*

$$1/I \sim \textit{Lognormal}(-\mu_{LN}, s_{LN}^2),$$

where μ_{LN} and s_{LN} are given by $\mu_{LN} = \log \sqrt{\frac{\mu_I^4}{\mu_I^2 + s_I^2}}$ and $s_{LN} = \sqrt{2}\sqrt{\log \frac{\sqrt{\mu_I^2 + s_I^2}}{\mu_I}}$.

Proof. First, approximate the normal distribution $\mathcal{N}(\mu_I, s_I^2)$ by a log-normal distribution $\text{Lognormal}(\mu_{\text{LN}}, s_{\text{LN}}^2)$ with mean μ_{I} and variance s_{I}^2. The inverse distribution is simply $\text{Lognormal}(-\mu_{\text{LN}}, s_{\text{LN}}^2)$. □

Consequently, the mean of $1/I$ is

$$\mathbb{E}[1/I] = \exp\{-\mu_{\text{LN}} + s_{\text{LN}}^2/2\} = \frac{\mu_{\text{I}}^2 + s_{\text{I}}^2}{\mu_{\text{I}}^3} \tag{12}$$

and the variance is

$$\begin{aligned} \mathbb{V}[1/I] &= \exp\{-2\mu_{\text{LN}} + s_{\text{LN}}^2\}(-1 + \exp\{s_{\text{LN}}^2\}) \\ &= \frac{s_{\text{I}}^2(\mu_{\text{I}}^2 + s_{\text{I}}^2)^2}{\mu_{\text{I}}^8}, \end{aligned} \tag{13}$$

where the mean μ_{I} and variance s_{I}^2 of the interference is given in (9) and (10).

C. Moments of ratio distribution

Should we know the distributions of P_{TX} and $1/I$, we can calculate the moments of the distribution of P_{TX}/I by algebra of random variables.

The mean of the ratio distribution P_{TX}/I is

$$\mathbb{E}[P_{\text{TX}}/I] = \mathbb{E}[P_{\text{TX}}]\mathbb{E}[1/I], \tag{14}$$

and the variance is

$$\begin{aligned} &\mathbb{V}[P_{\text{TX}}/I] = \mathbb{V}[P_{\text{TX}}] \cdot \mathbb{V}[1/I] + \\ &\mathbb{V}[P_{\text{TX}}] \cdot (\mathbb{E}[1/I])^2 + \\ &\mathbb{V}[1/I] \cdot (\mathbb{E}[P_{\text{TX}}])^2, \end{aligned} \tag{15}$$

where for generalized noncentral chi-squared distribution

$$\mathbb{E}[P_{\text{TX}}] = \nu_{\text{TX}}^2 + 2\sigma_{\text{TX}}^2, \tag{16}$$

and

$$\mathbb{V}[P_{\text{TX}}] = 4(\nu_{\text{TX}}^2\sigma_{\text{TX}}^2 + \sigma_{\text{TX}}^4), \tag{17}$$

and $\mathbb{E}[1/I]$ and $\mathbb{V}[1/I]$ are given in (12) and (13).

D. Distribution of SIR

Finally, we will derive the closed-form distribution for the SIR. The analysis is divided into two sections: for the non-LOS case ($K = 0$) in III-D1, and for the partial LOS ($K > 0$) in III-D2.

1) Rayleigh fading case: Assuming that the test transmitter signal is Rayleigh faded (i.e. Rician faded with parameter $K = 0$), i.e. the power is exponentially faded, we have according to the approximation (11):

$$\begin{aligned} \mathbf{P}[\text{SIR} \geq t] &= \mathbf{P}\left[\frac{P_{\text{TX}}}{I} \geq t\right] = \mathbf{P}\left[P_{\text{TX}} \geq tI\right] \\ &= \mathbb{E}_I\left[e^{-t/p_{\text{TX}} I}\right] = \mathcal{L}_I(t/p_{\text{TX}}) \\ &\approx e^{-\sum_i \lambda^{(i)} L^{(i)} \frac{p_I^{(i)}}{p_{\text{TX}}} t}. \end{aligned} \tag{18}$$

In other words, the SIR is exponentially distributed with rate $\mu_{\text{SIR}} = \sum_i \lambda^{(i)} L^{(i)} p_I^{(i)} / p_{\text{TX}}$ should there be no LOS between the test transmitter and the satellite.

2) General fading case: The gamma distribution is the conjugate prior of the exponential distribution. Thus, we propose that the distribution of SIR follows a gamma distribution in the general Rician fading case.

Gamma distribution depends on the shape parameter $k > 0$ and scale parameter $\theta > 0$. The mean is given by $k\theta$, and variance is given by $k\theta^2$. To approximate the distribution of SIR by the gamma distribution, we match the mean (14) and variance (15) to the corresponding moments of the Gamma distribution;

$$\begin{cases} k\theta = \mathbb{E}[\text{SIR}] = L(d)\mathbb{E}[P_{\text{TX}}/I] \\ k\theta^2 = \mathbb{V}[\text{SIR}] = L(d)\mathbb{V}[P_{\text{TX}}/I]. \end{cases} \tag{19}$$

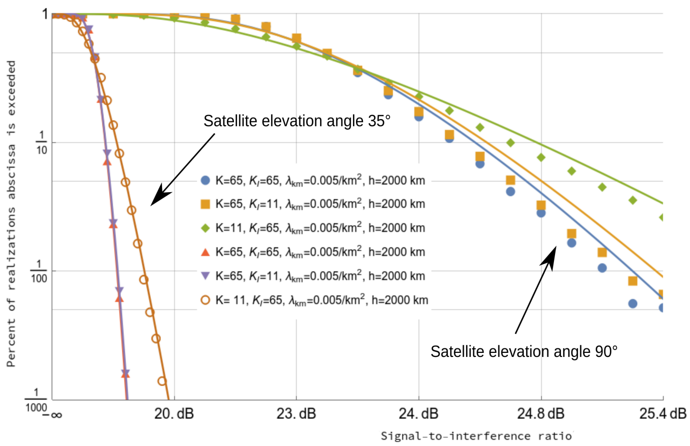

Fig. 2. Figure shows the simulated points of the complementary cumulative density function of SIR and the corresponding gamma distribution approximations. Satellite is at altitude $h = 2000$ km, and density of interferers $\lambda_{km} = 0.005/\text{km}^2$. Parameter K denotes the Rician parameter of the test transmitter, and K_I denotes the Rician parameter of the non-shadowed interferers. The density function diverges from the simulated values with elevation angle 90° as the mean number of interferers inside the 3 dB footprint is small ($\lambda_{3dB} \approx 10$), and the theory presented in this paper does not apply.

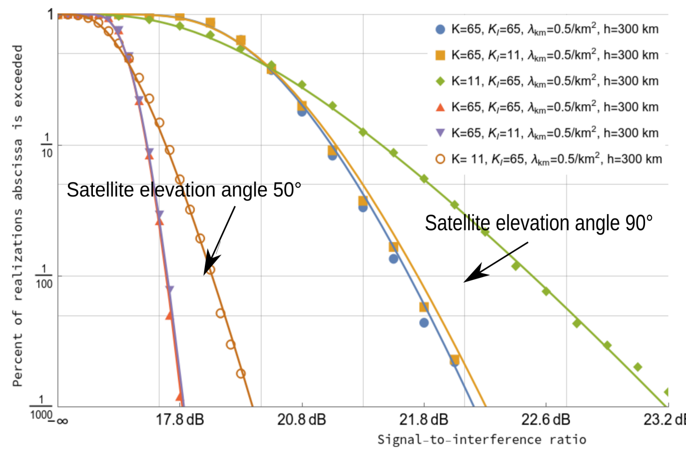

Fig. 3. Figure shows the simulated points of the complementary cumulative density function of SIR and the corresponding gamma distribution approximations. Satellite is at altitude $h = 300$ km, and density of interferers $\lambda_{km} = 0.5/\text{km}^2$. Parameter K denotes the Rician parameter of the test transmitter, and K_I denotes the Rician parameter of the non-shadowed interferers.

Solving the parameters k and θ and substituting (14) and (15), yields

Proposition 3 (Distribution of SIR)**.** *The distribution of SIR approximates the* ***gamma distribution*** $\Gamma(k, \theta)$ *with parameters*

$$
\begin{aligned}
k &= L(d)\mathbb{E}[P_{TX}/I]^2/\mathbb{V}[P_{TX}/I] \\
&= L(d)(\mathbb{E}[P_{TX}]\mathbb{E}[1/I])^2/\big(\mathbb{V}[P_{TX}]\cdot\mathbb{V}[1/I]+ \\
&\qquad \mathbb{V}[P_{TX}]\cdot(\mathbb{E}[1/I])^2+ \\
&\qquad \mathbb{V}[1/I]\cdot(\mathbb{E}[P_{TX}])^2\big),
\end{aligned} \tag{20}
$$

$$
\begin{aligned}
\theta &= \mathbb{V}[P_{TX}/I]/\mathbb{E}[P_{TX}/I] \\
&= \big(\mathbb{V}[P_{TX}]\cdot\mathbb{V}[1/I]+ \\
&\quad \mathbb{V}[P_{TX}]\cdot(\mathbb{E}[1/I])^2+ \\
&\quad \mathbb{V}[1/I]\cdot(\mathbb{E}[P_{TX}])^2\big)/\mathbb{E}[P_{TX}]\mathbb{E}[1/I],
\end{aligned} \tag{21}
$$

where the means $\mathbb{E}[\cdot]$ *and variances* $\mathbb{V}[\cdot]$ *are given for* P_{TX} *in* (16) *and* (17)*, and for* $1/I$ *in* (12) *and* (13).

IV. Results

We compare the derived gamma distribution approximation to Monte Carlo simulated values in the figures 2 and 3 with varying altitudes and elevation angles. The parameters for the gamma distribution are given in Proposition 3

In the theory, the Interfering transmitters are shadowed with probability $S = 0.44$ and are divided into to classes of non-shadowed transmitters and shadowed transmitter with densities $\lambda^{(1)} = (1 - 0.44)\lambda$ and $\lambda^{(2)} = 0.44\lambda$, respectively.

We consider that the path-loss function is equal to all transmitters. This implies that the path-loss function cancels itself out in the expression of SIR (2). In other words, the altitude or the elevation angle of the satellite does not affect the distribution of SIR should λ_{3dB} remain constant. The only parameters affecting the distribution of SIR are the mean transmitting powers and fading conditions.

The simulated values are acquired by Monte Carlo simulations by calculating an average over different realizations of the PPP and fading. In simulations, we use a Gaussian antenna as given in (3). Furthermore, an additive -84 dBm noise component is present.

A. Transmitter characteristics

We consider one type of omni-directional interfering transmitters transmitting with power 43 dBm. Shadowing is present at a probability 0.44, and the powers of the shadowed transmitters are reduced by 11 dBm. This leads us to two classes of interferers: shadowed and non-shadowed transmitters. Shadowed interferers experience Rayleigh fading, and non-shadowed interferers experience Rician fading with Rician parameter $K = 65$ or $K = 0$. Test transmitter power is 69.1 dBm, and it experiences Rician fading with $K = 65$ or $K = 11$.

In the results section, interfering transmitters' properties are set to mimic a realistic LEO network. The interfering transmitting powers follow FCC regulations for mobile interfaces operating in 28, 39, and 37 GHz bands in [16]. The fast and slow fading conditions follow the values given in the survey on terrestrial-satellite transmitters [17]. Path loss function $l(d) = (3.55d)^2$ and receiving satellites gain width follows the characteristics of a SpaceX constellation [18].

B. Remarks of the results

With small densities of interferers (inside the 3 dB footprint) (figure 2 elevation angle 90°), the approximation is reasonable, but the particularly the tail distribution diverges as seen in the figure 2. With high densities (figure 2 elevation angle 35°, and figure 3), the gamma distribution approximation matches very well. Depending also on the relative transmitting powers and densities in different classes of interferers, we suggest that ~ 10 interferers should be present so that the gamma function approximation is valid. The variance and skewness of the distribution increase with lower densities of interferers. However, the tails are not heavy-tailed (neither in simulations nor in gamma function approximation) in the sense that they decay faster than the exponential distribution. With high densities, the distribution of SIR is near to Gaussian distribution ($\Gamma(k,\theta) \rightarrow \mathcal{N}(k\theta, k\theta^2)$ as $k \rightarrow \infty$), should the Rician parameter K_{TX} of the test transmitter channel be above 0. With $K_{\text{TX}} = 0$, the distribution is always exponential, as stated in the analysis. Particularly, the tail probabilities are well approximated. In the figure 2, the mean number of interferers inside the 3 dB footprint is $\lambda_{3dB} \approx 10$ and $\lambda_{3dB} \approx 68$ for the elevation angles $90°$ and $35°$, respectively. In the figure 3, the mean number of interferers inside the 3 dB footprint is $\lambda_{3dB} \approx 24$ and $\lambda_{3dB} \approx 68$ for the elevation angles $90°$ and $50°$, respectively.

The SIR is smaller with low satellite elevation angles if the density of interferers and transmitter powers are kept constant; approximately 5 dB and 2 dB variation is present in the figures 2 and 3, respectively. Furthermore, the altitude and elevation angle have crucial effect on the distribution of SIR. This is due to the widening of the footprint of the satellite that causes more interferers to be present inside the main lobe. It is clear that satellite receiver in the lower altitudes tolerate more interferers than a receiver in the high altitudes. However, at $h = 300$km, the lower elevation angles of the satellite causes the SIR to drop to zero with the density parameter $\lambda_{km} = 0.5$. In this context, the gamma distribution approximation of SIR can be used to study the power control in a terrestrial-satellite link.

The test transmitter fading conditions transmitter has bigger effect on the SIR distribution than fading conditions of the interferers.

The analysis presented does apply only for small footprints as for large footprints the interferers are further away and the mean interference is smaller considering that the same mean amount of interferers is present. In this paper, the theory was tested against a Gaussian antenna, and the theory was shown to work in this case well.

V. Conclusion

We derived gamma distribution approximation for the distribution of SIR in a terrestrial-satellite link. The approximation is applicable when the receiver antenna beam pattern is narrow and the density of interferers is large. With smaller densities, the interference will become impulsive as there is a high chance of having no interferers inside the receiving satellite's main lobe. We suggest that the gamma distribution is a good approximation when there are 10 interferers on average – or more – inside the satellite's 3 dB footprint. The $1.5°$ 3 dB beamwidth of the receivers used in this paper is sufficiently narrow for the approximation to work. We conclude that the gamma distribution can be used as a prior distribution for the SIR in a terrestrial-satellite uplink in highly populated areas, such as cities, where dense (possibly heterogeneous) networks are causing additive co-channel interference.

The closed form SIR distribution presented in this paper is straightforward to derive and applies to various fading conditions and transmitter characteristics as well as different altitudes and elevation angles of a LEO satellite. Furthermore, overlapping heterogeneous interfering networks can be considered. A downside is that the transmitters have to be considered to be Poisson distributed, that is, completely independently located. Furthermore, only omni-directional antenna patterns for the interferers was considered. However, these are realistic assumptions particularly in the case of mobile user devices.

References

[1] D. Middleton, "Statistical-physical models of electromagnetic interference," *IEEE Transactions on Electromagnetic Compatibility*, vol. EMC-19, no. 3, pp. 106–127, 1977.

[2] K. Gulati, B. L. Evans, J. G. Andrews, and K. R. Tinsley, "Statistics of co-channel interference in a field of poisson and poisson-poisson clustered interferers," *IEEE Transactions on Signal Processing*, vol. 58, no. 12, pp. 6207–6222, 2010.

[3] X. Yang and A. Petropulu, "Co-channel interference modeling and analysis in a poisson field of interferers in wireless communications," *IEEE Transactions on Signal Processing*, vol. 51, no. 1, pp. 64–76, 2003.

[4] J. Ilow and D. Hatzinakos, "Analytic alpha-stable noise modeling in a poisson field of interferers or scatterers," *IEEE Transactions on Signal Processing*, vol. 46, no. 6, pp. 1601–1611, 1998.

[5] G. Samorodnitsky and M. S. Taqqu, *Stable Non-Gaussian Random Processes: Stochastic Models with Infinite Variance: Stochastic Modeling*. Routledge, 2017.

[6] K. Gulati, B. L. Evans, and K. R. Tinsley, "Statistical modeling of co-channel interference in a field of poisson distributed interferers," in *2010 IEEE International Conference on Acoustics, Speech and Signal Processing*, pp. 3490–3493, 2010.

[7] R. W. Heath, M. Kountouris, and T. Bai, "Modeling heterogeneous network interference using poisson point processes," *IEEE Transactions on Signal Processing*, vol. 61, no. 16, pp. 4114–4126, 2013.

[8] P. Madhusudhanan, J. G. Restrepo, Y. Liu, and T. X. Brown, "Carrier to interference ratio analysis for the shotgun cellular system," in *GLOBECOM 2009 - 2009 IEEE Global Telecommunications Conference*, pp. 1–6, 2009.

[9] N. Okati, T. Riihonen, D. Korpi, I. Angervuori, and R. Wichman, "Downlink coverage and rate analysis of low earth orbit satellite constellations using stochastic geometry," *IEEE Transactions on Communications*, vol. 68, no. 8, pp. 5120–5134, 2020.

[10] N. Okati and T. Riihonen, "Stochastic analysis of satellite broadband by mega-constellations with inclined LEOs," in *2020 IEEE 31st Annual International Symposium on Personal, Indoor and Mobile Radio Communications*, pp. 1–6, 2020.

[11] A. Yastrebova, I. Angervuori, N. Okati, M. Vehkaperä, M. Höyhtyä, R. Wichman, and T. Riihonen, "Theoretical and simulation-based analysis of terrestrial interference to LEO satellite uplinks," in *GLOBECOM 2020 - 2020 IEEE Global Communications Conference*, pp. 1–6, 2020.

[12] B. A. Homssi and A. Al-Hourani, "Modeling uplink coverage performance in hybrid satellite-terrestrial networks," *IEEE Communications Letters*, vol. 25, no. 10, pp. 3239–3243, 2021.

[13] B. Di, L. Song, Y. Li, and H. V. Poor, "Ultra-dense LEO: Integration of satellite access networks into 5g and beyond," *IEEE Wireless Communications*, vol. 26, no. 2, pp. 62–69, 2019.

[14] B. B. François Baccelli, *Stochastic Geometry and Wireless Networks*, vol. 1. NoW Publishers, 2009.

[15] E. Díaz-Francés and F. J. Rubio, "On the existence of a normal approximation to the distribution of the ratio of two independent normal random variables," *Statistical Papers*, 2013.

[16] F. C. Commission, "Report and order and further notice of proposed rulemaking," tech. rep., Federal Communications Commission, 2016.

[17] E. Lutz, D. Cygan, M. Dippold, F. Dolainsky, and W. Papke, "The land mobile satellite communication channel-recording, statistics, and channel model," *IEEE Transactions on Vehicular Technology*, vol. 40, no. 2, pp. 375–386, 1991.

[18] M. Albulet, "Spacex v-band non-geostationary satellite system," tech. rep., Space Exploration Technologies Corp., 2017.